Mathematical Model of the Arctic Gyre and its Analysis

Exploring the behaviour of a non-linear ordinary differential equation describing the vorticity of Arctic Gyres

S.P.T. Wiechers

TU Delft

Mathematical Model of the Arctic Gyre and its Analysis

Exploring the behaviour of a non-linear ordinary differential equation describing the vorticity of Arctic Gyres

by

S.P.T. Wiechers

to obtain the degree of Bachelor of Science
at the Delft University of Technology,
to be defended publicly on Wednesday June 26, 2024 at 12:00

Student number:	4948262	
Project duration:	April 25 2024 – June 26, 2024	
Thesis committee:	Dr.Kateryna Marynets	TU Delft, supervisor
	Dr.Cornelis Kraaikamp	TU Delft

An electronic version of this thesis is available at `http://repository.tudelft.nl/`.

TU Delft

Preface

"I would like to thank Dr. Kateryna Marynets for her help and guidance during the project, as well as Dr. Cornelis Kraaijkamp for being part of my graduation committee."

S.P.T. Wiechers
Delft, June 2024

Contents

List of Variables

Variable	Description	Dependencies
ψ	Represents the stream function in fluid dynamics, used to describe the flow of a fluid in a two-dimensional incompressible flow.	directional components (x,y),(θ,ϕ), r or t
x	Directional component describing horizontal location	
y	Directional component describing vertical location	
u	The velocity of the fluid in the x-direction	
v	The velocity of the fluid in the y-direction	
θ	Angle measured from the polar axis, used in spherical coordinates.	
ϕ	Angle measured around the polar axis, used in spherical coordinates.	
ω	Parameter that accounts for the Coriolis effect due to the Earth's rotation, influencing the fluid's movement. The value equals 4649.56.	
$u(t)$	Vorticity function in terms of variable t.	Depends on t
$F(u(t))$	Function representing the vorticity of the ocean flow, which is a measure of the rotation of fluid particles.	Depends on $u(t)$
r	Distance from the origin in spherical coordinates.	
t	A spatial variable	
t_0	Initial value of the spatial variable.	
ξ	Complex coordinate used in stereographic projection to map points on a sphere.	
Δ	Differential operator given by the divergence of the gradient of a function, important in describing the flow.	
ϵ	Parameter used to scale the impact of the oceanic vorticity function.	
λ_n	Value characterizing the eigenfunctions in the eigenvalue problem.	Dependent on the form of the differential equation
ϕ_n	Function corresponding to the eigenvalue in the eigenvalue problem, non-zero and orthogonal.	Dependent on λ_n
M	Constant used in depicting upper bounds	
Ψ	Component of the stream function related specifically to the vorticity.	Dependent on ψ
$\mathbb{R}$	Standard mathematical set of real numbers.	
$\mathbb{N}$	Standard mathematical set of natural numbers.	
X, Y	Abstract spaces in which distance is defined.	
d_X, d_Y	Distance measures defined on the metric spaces X and Y.	Dependent on X, Y

Laymen Summary

In the world there are five primary oceanic gyres: the North Atlantic, South Atlantic, North Pacific, South Pacific, and Indian Ocean gyres. These gyres are bounded by the continents and are driven by the wind patterns associated with Earth's climate [9]. Besides these large gyres, there exist smaller gyres near the North and South Pole. This paper will specifically be delve into the behaviour of Arctic gyres. These gyres are large systems of circulating ocean currents that play a crucial role in regulating the planet's climate by redistributing heat from the equator to the poles and supporting marine life. The main goal of this report is to explore and expand a mathematical equation, that was first presented by Constantin and Johnson [4], and later simplified by Jifeng Chu [3], to model Arctic gyres in particular.

The model uses complex equations to describe the vorticity of these Arctic gyres. Vorticity is a concept in fluid dynamics describing the rotation of fluid particles. In Chu's paper [3], the author preforms an analysis of the oceanic vorticity component within the model. The focus of this analysis lies predominantly in proving that there exist unique functions describing Arctic gyres, when the oceanic vorticity function has certain properties.

By extending the model, this report shows that different properties of the oceanic vorticity function, than those discussed by Chu [3], can also yield functions describing these gyres. Moreover, an analysis of scaling the oceanic vorticity component by a parameter $\epsilon > 0$, yields unstable results. These findings indicate how the original model can use different vorticity functions to correctly model Arctic gyres.

Summary

Arctic gyres are large systems of circulating ocean currents that form in the polar region. They play a crucial role in Earth's climate system by redistributing heat from the equator to the poles, facilitating the exchange of nutrients and gases between the ocean and atmosphere, and supporting marine ecosystems. Modeling Arctic gyres is important for understanding their impact on global climate patterns and predicting changes in marine environments. In 2017, A. Constantin and R.S. Johnson presented a shallow-water model [4], in which the authors derived a partial differential equation (PDE) describing gyres. Hereafter, in 2018, Jifeng Chu simplifies this model using the stereographic projection to rewrite this PDE into an ordinary differential equation (ODE)[3]. The present report investigates and expands this mathematical model describing Arctic gyres.

A key characteristic of this model is vorticity, a measure of the rotation of fluid particles. In particular, Chu's work [3] focuses on analysing the oceanic vorticity component: $F(u)$, in the model describing Arctic gyres. This analysis shows that there exists a unique continuous function describing the vorticity of an Arctic gyre, if $F(u)$ is a Lipschitz-continuous function. The results in this paper indicate that the model has continuous solutions for function $F(u)$ that are bounded. Additionally, numerical approximations of solutions to the differential equation validate that the model converges to a specific starting parameter and can effectively handle non-Lipschitz continuous functions. Furthermore the stability of the system is tested when the oceanic vorticity function $F(u)$ is scaled by a parameter ϵ. This analysis shows for linear functions $F(u) = au + b$, where a, b are real valued constants, that there exist no unique solutions whenever there is a $n \in \mathbb{N}$, such that $\epsilon = \frac{n(n-1)}{a}$.

Overall, the findings that are presented, highlight the potential for extending the model to incorporate more complex and realistic oceanic vorticity functions. This can improve the understanding of these crucial components of Earth's climate system.

1 Introduction

Ocean gyres are large systems of circulating ocean currents formed by the interaction of wind patterns and the Earth's rotation (the Coriolis effect). These gyres can span entire ocean basins and are a dominant feature of the Earth's oceanic circulation. There exist five major gyres: the North- and South Atlantic Gyre, the North- and South Pacific Gyre, and the Indian Ocean Gyre, as well as smaller gyres in the Arctic and Antarctic region. Gyres are characterized by a central area of calm water and a strong, circular flow around the periphery. They play a crucial role in the global climate system by redistributing heat from the equator to the poles and facilitating the exchange of nutrients and gases between the ocean and the atmosphere[9]. The motion of these currents is driven primarily by wind stress at the ocean surface, but the Coriolis effect also plays a significant role, causing the currents to turn and form a circular pattern. In the Northern Hemisphere, gyres rotate clockwise, while in the Southern Hemisphere, they rotate counterclockwise. These oceanic features are not only vital for regulating global climate but also support marine ecosystems by distributing nutrients and supporting the migration patterns of various marine species. The study of gyres, particularly in the polar regions, is essential due to their influence on sea ice dynamics, their role in global heat circulation, and their impact on regional climate patterns. This report aims to explore the non-linear model presented by Jifeng Chu [3] describing Arctic gyres, exploring the mathematical formulations and delve deeper into possible extensions and stability of the model.

Jifeng Chu's 2018 paper, "On a nonlinear model for arctic gyres," published in the Annali di Matematica, starts with a model given by Constantin and Johnson [4], where the authors describe circulation of the water mass in the ocean as a shallow-water problem. Chu's work begins by simplifying the partial differential equation model presented in [4], into a second order ordinary differential equation. This model provides significant insights into the dynamics of ocean gyres, specifically in the Arctic region.

The Arctic Ocean's unique conditions, such as wind stress factors and the influence of the Coriolis effect, give rise to specialized models to accurately describe the gyre's motion. Chu's work highlights the transformation of the spherical coordinate model into a planar elliptic boundary value problem, which simplifies the analysis while retaining the essential physical characteristics of the gyre. By neglecting azimuthal variations and focusing on radially symmetric solutions, using stereographic projection, the model becomes more manageable, while still providing a useful framework for investigating these systems

This report will explore and extend Chu's work by researching different properties of the nonlinear model, as well as providing stability and bifurcation analysis. The second chapter focuses on the exploration of the model. This translates to the background information, theorems and general information. The section thereafter will give insight into the simplification of the model given by Constantin and Johnson [4] towards the model that is used in the paper by J.Chu. Moreover, the results regarding the extension, and analysis of the model will also be discussed. The last chapter of the report gives a conclusion and a possible discussion, which summarises the report and gives possible recommendations for further research.

2

Literary study

To understand the results given by J.Chu [3], one must have some basic understanding of the origin of the nonlinear model, as well as some results that arise in the field of real analysis and ordinary differential equations. This chapter will provide some background information concerning the derivation of the model and related theorems, used for its analysis.

2.1. Introduction to Ocean Gyres

Ocean gyres are vast, circulating ocean currents, that dominate the surface circulation in the major ocean basins. There are five primary oceanic gyres: the North Atlantic, South Atlantic, North Pacific, South Pacific, and Indian Ocean gyres. These gyres are bounded by the continents and are driven by the wind patterns associated with Earth's climate [9].

2.1.1. Formation of Oceanic Gyres

The primary drivers of oceanic gyres are wind patterns and the Coriolis effect, which work together to create the characteristic circular motion of gyres. Trade winds blow from east to west in the tropics, while the westerlies blow from west to east in the mid-latitudes. These westerlies and easterlies create a pattern of surface currents that converge and diverge, setting up the circular motion characteristic of gyres,leading to the formation of gyres [9].

2.1.2. The Coriolis effect

The Coriolis effect is a phenomenon that describes the apparent deflection of objects moving across the surface of the Earth, due to the planet's rotation. Named after the French mathematician Gaspard-Gustave de Coriolis, this effect is crucial in meteorology and oceanography for understanding the movement patterns of air and water currents. As the Earth rotates, different points on the planet move at different speeds. The Earth is at its widest at the Equator, therefore regions near the Equator travel faster relative to regions near the poles. When an object travels long distances over the Earth's surface, such as an air current or an ocean current, it retains its initial speed relative to Earth's rotation. However, as it moves to areas where the ground speed is different, it appears to curve. This deflection to the right in the Northern Hemisphere and to the left in the Southern Hemisphere is the Coriolis effect[7].

2.2. Origin of the model for Arctic gyres

The nonlinear model for gyres derived by Constantin and Johnson [4] begins by formulating oceanic flow in spherical coordinates. This implies the coordinate system of a polar angle θ from 0 to π, representing the South and North pole respectively. As well as an azimuthal angle ϕ ranging from 0 to 2π, corresponding to the angle of longitude. The horizontal flow on the spherical Earth corresponding to a gyre is described in terms of $\psi(\theta,\phi)$, the stream function.

2.2.1. The Stream function and Vorticity

In fluid dynamics, the stream function ψ is a critical tool used to describe the flow of an in-compressible fluid in two dimensions. One of the essential properties of the stream function is that it ensures mass conservation. This is mathematically expressed by the continuity equation, which for an in-compressible flow in the xy-plane is given by

$$\frac{\partial u}{\partial x} + \frac{\partial v}{\partial y} = 0.$$

Here, u and v are the velocity components of the fluid in the x and y directions respectively,

$$u = \frac{\partial \psi}{\partial y}, v = -\frac{\partial \psi}{\partial x}.$$

The continuity equation is automatically satisfied, since

$$\frac{\partial u}{\partial x} = \frac{\partial^2 \psi}{\partial y \partial x}, \quad \frac{\partial v}{\partial x} = -\frac{\partial^2 \psi}{\partial y \partial x}$$

implies

$$\frac{\partial u}{\partial x} + \frac{\partial v}{\partial x} = \frac{\partial^2 \psi}{\partial y \partial x} - \frac{\partial^2 \psi}{\partial y \partial x} = 0.$$

Using spherical coordinates (θ, ϕ), the velocity components (u, v) are expressed as

$$u_\phi = \frac{1}{\sin(\theta)} \frac{\partial \psi}{\partial \phi}, u_\theta = -\frac{\partial \psi}{\partial \theta}.$$

To further analyse the motion of the gyre, the stream function $\psi(\theta, \phi)$ is decomposed into two parts:

$$\psi(\theta, \phi) = -\omega \cos(\theta)) + \Psi(\theta, \phi),$$

where ω is the Coriolis parameter and Ψ is associated with the oceanic vorticity. Vorticity is a measure of the rotation of a fluid and is defined as the curl of the velocity.[1]. This measure has two components, one for the absolute rotation of the Earth, and one with respect to the fluid, relative to the rotation of the Earth. The vorticity describes both the rotation and direction of a fluid parcel. In the case for modeling gyres, Ψ is connected to the vorticity of the underlying motion of the ocean with governing equation

$$\frac{1}{\sin^2 \theta} \frac{\partial^2 \Psi}{\partial \phi^2} + \frac{\partial}{\partial \theta} \left(\cot \theta \frac{\partial \Psi}{\partial \theta} \right) + \frac{\partial^2 \Psi}{\partial \theta^2} = F(\Psi - \omega \cos \theta). \tag{2.1}$$

Note that the vorticity of the flow consist of two distinct components. The first are given by $2\omega \cos(\theta)$, describing the rotation of the Earth. The second is the oceanic vorticity, $F(\Psi - \omega \cosh(\theta)$, which has Earth's spin as a variable. This equation can be rewritten into a semi-linear elliptic equation using the stereographic project.

2.2.2. Stereographic projection

Stereographic project is a method of mapping a point on a sphere onto a plane. This projection is particularly useful in various fields such as cartography, complex analysis and, notably, fluid dynamics, as it often simplifies the analysis of spherical problems. Moreover, the mapping of the stereographic projection has the property that it preserves angles[6]. To visualize this projection, consider a sphere centered at the origin with a radius R. The projection is typically performed from the North Pole of the sphere onto the plane passing though the equator. Figure (2.1) below will give a visual idea of the map.

Note, while usually the projection is made form the North pole, the model presented in [3] makes use of a projection form the South Pole.

In the model for Arctic gyres, the projection plays a crucial role in deriving the nonlinear ordinary differential equation that models the motion of the gyre, given its property that it reduces to the system of one dimension less than the original. The projection maps the spherical coordinates (r, θ, ϕ) to the points (x, y) in a two dimensional plane[4], by taking

$$r = \cot(\frac{\theta}{2}), \quad x = r \cos(\phi), \quad y = r \sin(\phi)$$

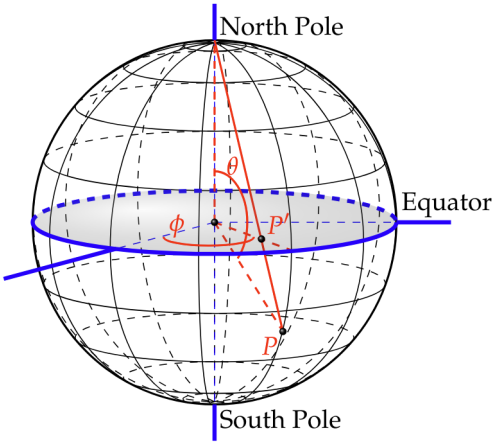

Figure 2.1: Illustration of the stereographic projection from the North pole onto the equatorial plane[6]

from which follows

$$\theta = 2arccot(r), \quad r = \sqrt{x^2+y^2}.$$

Furthermore define

$$\xi = re^{i\phi} \quad \text{with} \quad r = \cot\left(\frac{\theta}{2}\right) = \frac{\sin\theta}{1-\cos\theta}.$$

where (r,ϕ) are the polar coordinates in the equatorial plane. This gives

$$\cos\theta = \frac{\xi\bar{\xi}-1}{\xi\bar{\xi}+1}, \quad \sin\theta = \frac{\sqrt{\xi\bar{\xi}}}{\xi\bar{\xi}+1}, \quad \partial_\theta = -\frac{\xi}{\sin\theta}\partial_\xi - \frac{\bar{\xi}}{\sin\theta}\partial_{\bar{\xi}}, \quad \partial_\phi = i\xi\partial_\xi - i\bar{\xi}\partial_{\bar{\xi}}.$$

Applying these to the governing equation

$$\frac{1}{\sin^2\theta}\frac{\partial^2\Psi}{\partial\phi^2} + \cot\theta\frac{\partial\Psi}{\partial\theta} + \frac{\partial^2\Psi}{\partial\theta^2} = F(\Psi - \omega\cos\theta)$$

Constantin and Johnson [4] rewrite this equation into

$$\partial_{\xi\bar{\xi}}\psi + 2\omega\frac{1-\xi\bar{\xi}}{(1+\xi\bar{\xi})^3} - \frac{F(\psi)}{(1+\xi\bar{\xi})^2} = 0.$$

Or, using the points (x,y) as Cartesian coordinates in the complex ξ-plane, one finds

$$\Delta\psi + 8\omega\frac{1-(x^2+y^2)}{(1+x^2+y^2)^3} - \frac{4F(\psi)}{(1+x^2+y^2)^2} = 0 \tag{2.2}$$

where $\Delta = \partial_x^2 + \partial_y^2$ is the Laplace operator.

2.2.3. Simplification of the model to the second order differential equation

As seen, one is able to model gyres on the xy-plane $\mathcal{O}$ using stereographic projection. To simplify this even further towards the modeling of Arctic gyres specifically, one can look at the interval $\theta \in [\frac{14\pi}{15}, \pi]$, corresponding to the area surrounding the North pole. Note that in this region $r = \cot(\frac{\theta}{2}) < e^{-2}$. For the Arctic gyres a simplification is made such that the flow velocity has no azimuthal variation, provided that $\psi = \psi(r)$ is radially symmetric. Setting $t_0 = \ln(r_0) \geq 2$, $r = e^{-t}$ and $\psi_0 = u(t)$,with $t \geq t_0$, the model can be simplified using change of variables [3]. Note that in this particular case t is not time-dependent, but a spacial variable.
Let $r = e^{-t}$, and consider the Laplacian $\Delta\psi$ with respect to $r = \sqrt{x^2+y^2}$, then

$$\Delta\psi = \frac{\partial^2\psi}{\partial r^2} + \frac{1}{r}\frac{\partial\psi}{\partial r}$$

Using the change of variable $r = e^{-t}$, one finds the derivatives relative to t:

$$\frac{\partial \psi}{\partial r} = \frac{\partial \psi}{\partial t}\frac{\partial t}{\partial r} = -e^{-t}\frac{\partial \psi}{\partial t}$$

and similarly

$$\frac{\partial^2 \psi}{\partial r^2} = \frac{\partial^2 \psi}{\partial t^2}\left(\frac{\partial t}{\partial t}\right)^2 + \frac{\partial^2 t}{\partial r^2}\frac{\partial \psi}{\partial t} = e^{-2t}\frac{\partial^2 \psi}{\partial t^2} + e^{2t}\frac{\partial \psi}{\partial t}$$

Combining these into equation(2.2) with $\psi(r) = u(t)$ yields

$$e^{2t}u"(t) + 8\omega\frac{1-e^{-2t}}{(1+e^{-2t})^3} - F(\psi)\frac{4}{(1+e^{-2t})^2}.$$

Next consider

$$\sinh(t) = \frac{1-e^{-2t}}{2e^{-t}} \quad \text{and} \quad \cosh(t) = \frac{1+e^{-2t}}{2e^{-t}}.$$

Implementing these and multiplying by e^{-2t} gives the differential equation stated in [3], given by

$$u''(t) = \frac{F(u(t))}{\cosh^2(t)} - 2\omega\frac{\sinh(t)}{\cosh^3(t)}; t \geq t_0. \tag{2.3}$$

This equation forms the basis for the rest of the research stated in the report. Note that t in unbounded in this equation. This is due to the fact that the stereographic project exerts to infinity when nearing the pole. This property can give complications when numerically modeling the stream of the gyre.

2.3. Solution to the model

Using some basic methods from ordinary differential equations, abbreviated to ODE, the author of the paper [3] shows that the integration of the differential equation

$$u''(t) = \frac{F(u(t))}{\cosh^2(t)} - 2\omega\frac{\sinh(t)}{\cosh^3(t)}$$

over the interval $[t,\infty)$ yields

$$u'(t)|_t^\infty = \frac{\omega}{\cosh^2(t)} + \int_t^\infty \frac{F(u(s))}{\cosh^2(s)}ds.$$

With physical restraint $\lim_{t\to\infty}(u'(t)\cosh(t)) = 0$ this results in

$$-u'(t) = \frac{\omega}{\cosh^2(t)} + \int_t^\infty \frac{F(u(s))}{\cosh^2(s)}ds.$$

Taking the integral of both sides over the same interval gives

$$\lim_{t\to\infty}(-u(t)) + u(t) = -\omega + \omega\tanh(t) + \int_t^\infty\int_t^\infty \frac{F(u(s))}{\cosh^2(s)}ds$$

which equals

$$u(t) = [\psi_0 - \omega] + \omega\tanh(t) + \int_t^\infty (s-t)\frac{F(u(s))}{\cosh^2(s)}ds \tag{2.4}$$

Here, the boundary condition $\lim_{t\to\infty} u(t) = \psi_0$, as stated in [3], is used. This equation shows a result for the ODE, equation (2.3), describing the motion of the Arctic gyre. Note that this has only feasible solutions if

$$\int_t^\infty (s-t)\frac{F(u(s))}{\cosh^2(s)}ds$$

is bounded.

2.4. Oceanic Vorticity F(u) and Lipschitz-Continuity

F(u) is a nonlinear function that encapsulates the complex interactions of forces within the ocean. It typically depends on various factors such as the Earth's rotation, and the geometry of the ocean basin in which the gyres are located. The model displayed in Constantin and Johnson [4], however, is derived as a shallow-water model. Therefore only the wind and Coriolis effect have an impact on the gyre. The specific form of $F(u)$ can vary depending on the particular physical scenario being modeled. In general a goal is to select a $F(u)$ that accurately represents the oceanic vorticity dynamics of the gyre. In the paper of J.Chu [3] a proof is given for the existence and uniqueness of functions of $F(u)$ that are Lipschitz-continuous. The proof rests on the definition of Lipschtiz-continuity and Banach's fixed point theorem. These definitions and proofs are given in the succeeding sections.

2.4.1. Lipschitz-Continuity

Lipschitz-continuity is a powerful property within mathematics. A function $F(u) : X \to Y$, for two metric spaces (X, d_X) and (Y, d_Y), is said to have this property if there exists a constant $M \in \mathbb{R}^+$ such that for two values u, v in the domain of F

$$d_X(F(u), F(v)) \leq M d_Y(u, v)$$

holds. Here d_X and d_Y are the relative measures for sets X and Y, and $M \in \mathbb{R}$ is a constant. In words this implies that the distance between two functions $F(u)$ and $F(v)$ has no relatively rapid change. For real valued functions this translates into a function $F : R \to R$. with

$$|F(u) - F(v)| \leq M|u - v|.$$

The condition of Lipschitz-continuity is stronger then just continuity.

2.4.2. Existence and uniqueness to the problem for Lipschitz-continuous $F(u)$

Since the nonlinear ODE, written in equation (2.3), models a real world problem, one would expect that the values of the stream function $u(t)$, for $t \in [t_0, \infty)$, need to be bounded to be used in a physical model. Note that the existence of $u(t)$ depends on the choice of $F(u)$. In [3] a proof is given using Banach's fixed point theorem[8]. To explain this theorem, let (X, d) be a complete metric space, and denote $T : X \to X$ a map. By definition, a mapping $T : X \to X$ on a Banach space $(X, \|\cdot\|)$ is called a contraction mapping if there exists a constant $0 \leq k < 1$ such that for all $x, y \in X$:

$$\|T(x) - T(y)\| \leq k\|x - y\|.$$

Here, k is known as the contraction constant. This condition ensures that T brings points closer together, meaning that the distance between the images of two points under T is strictly less than the distance between the points themselves, scaled by the factor k. Banach's fixed point theorem states that, if the mapping of $T : X \to X$ is a contraction mapping, then T has a unique fixed point $x \in X$.To translate this to the nonlinear model (equation (2.3), consider its solution, derived in section 2.3 and presented in [2]:

$$u(t) = [\psi_0 - \omega] + \omega \tanh(t) + \int_t^\infty (s - t) \frac{F(u(s))}{\cosh^2(s)} ds.$$

Next, consider the map $\mathscr{F} : X \to X$, where X is a Banach space of all continuous and bounded functions $u : [t_0, \infty) \to \mathbb{R}$, with norm $||u|| = sup_{t \geq t_0}\{|u|\}$. Here the operator $\mathscr{F}$ is denoted as:

$$[\mathscr{F}(u)](t) = [\psi_0 - \omega] + \omega \tanh(t) + \int_t^\infty (s - t) \frac{F(u(s))}{\cosh^2(s)} ds.$$

Suppose there exist two continuous solutions $u, v : [T_0, \infty) \to \mathbb{R}$ to equation (2.3), then the distance between these two solutions is

$$||\mathscr{F}(u) - \mathscr{F}(v)|| \leq \sup_{t \geq T_0} \int_t^\infty (s - t) \frac{|F(u) - F(v)|}{\cosh^2(s)} ds.$$

Note that F is Lipschitz-continuous, therefore there exists $M \in \mathbb{R}$, such that

$$|F(u) - F(v)| \leq M|u - v|.$$

Applying this yields

$$\sup_{t\geq T_0}\int_t^\infty (s-t)\frac{|F(u)-F(v)|}{\cosh^2(s)}ds \leq \sup_{t\geq T_0}\int_t^\infty (s-t)\frac{M|u-v|}{\cosh^2(s)}ds.$$

$$\leq M||u-v||\sup_{t\geq T_0}\int_t^\infty \frac{s-t}{\cosh^2(s)}ds$$

Using $s, t \geq 0$, then $\sinh(s) \geq s \geq s-t$, gives

$$M||u-v||\sup_{t\geq T_0}\int_t^\infty \frac{\sinh(s)}{\cosh^2(s)}ds = \frac{M}{\cosh(T_0)}M||u-v||.$$

Choosing T_0 such that $\cosh(T_0) \geq M$, this indeed gives a contraction mapping. Thus $\mathscr{F}(u)$ provides a unique continuous solution $u(t) : [t_0, \infty)$ if $t_0 = T_0$. Moreover, J.Chu [2] shows that this implies for all t_0 using the Lipschitz-continuity of $F(u)$. The following chapter uses the theorems and definitions given in these sections to expand the work of J.Chu in [3] and [2].

3

Methods, Results and Analysis

Understanding and extending the differential equation (2.3) used to model the Arctic gyre [3] requires mathematical skills and the application of various theorems. This chapter will detail the methods employed to achieve these extensions and provide an analysis of the results that are found.

3.1. Methods

This section focuses on the methods and techniques used to extend the work of J.Chu. The model has been expanded in three directions. The first is the search for functions of the oceanic vorticity $F(u)$, that are not Lipschitz-continuous, but do have real, physically relevant solutions to the ODE (2.3), modeling Arctic gyres. The second is concerned with numerically modeling the behaviour of the nonlinear ordinary differential equation [3]. Lastly the effects of scaling $F(u)$ with a parameter $\epsilon \in \mathbb{R}$ are considered.

3.1.1. Non Lipschitz-continuous functions of F(u)

There has been given a rigorous proof stating the existence and uniqueness of a solution $u : [t_0, \infty) \to \mathbb{R}$ when the oceanic vorticity $F(u)$ is Lipschitz-continuous. However, real oceanic flows are influenced by a multitude of factors including wind and transient effects due to the climate variability. These factors can result in vorticity functions that exhibit rapid changes, or have non-linear behaviour. By considering non-Lipschitz continuous functions, one can better capture the true complexity of ocean dynamics. When solving the differential equation in [3] it is important to note that $u(t)$ describes a physical system, namely the vorticity in the Arctic gyre. Therefore the solution to $u(t)$ is expected to be bounded for every $t \in [t_0.\infty)$.

3.1.2. Numerical analysis

There are multiple approaches used in numerical analysis to solve differential equations. It is possible to analyse the entire differential equation

$$u"(t) = \frac{F(u)}{\cosh^2(t)} - \frac{2\omega \sinh(t)}{\cosh^3(t)}$$

as a boundary value problem using a finite difference method. However, Jifeng Chu [3] has already given a nonlinear result for $u(t)$ (equation (2.4)), which contains an improper integral. Using this analytic notation of the solution $u(t)$, a python code (Appendix A.1) can be written that makes use of an expected fixed value to the function $u(t)$, for a given $t \in [t_0, N]$, where N is a large integer representing infinity. Here it is wise to note that using infinity in a numerical approach can cause for some problems or inconsistencies.

3.1.3. Stability analysis of scaling $F(u)$ by parameter ϵ

In the abstract of Jifeng Chu[3], there are many examples for solutions to oceanic vorticity functions $F(u)$ that are linear combinations of $u(t)$. However, one can wonder if it is possible to take different or more complex values for this oceanic vorticity function. By multiplying $F(u)$ by a parameter $\epsilon \in \mathbb{R}$, the possibility arises to scale the impact that $F(u)$ has on the system. Implementing this parameter yields the following differential

equation.

$$u''(t) = \frac{\epsilon F(u)}{\cosh^2(t)} + \frac{2\omega \sinh(t)}{\cosh^3(t)}. \tag{3.1}$$

The following sections will discuss the existence, uniqueness and stability of solutions to equation (3.1). This is done by rewriting equation (3.1) into a well studied Sturm-Liouville eigenvalue problem, with known eigenvalues, using a change of variables. If such a problem is found, theorems involving eigenvalues and eigenfunctions, can be used to indicate or refute the aforementioned properties of possible solutions. To write an equation into a Sturm-Liouville eigenvalue problem, consider the following differential equation:

$$a_2(x)y'' + a_1(x)y' + a_0(x)y = f(x),$$

where $a_2(x)$, $a_1(x)$, and $a_0(x)$ are given coefficient functions, and $f(x)$ is a given function. This can be written in the form

$$\frac{d}{dx}\left(p(x)\frac{dy}{dx}\right) + q(x)y = F(x)$$

where

$$\begin{aligned} p(x) &= e^{\int \frac{a_1(x)}{a_2(x)}\,dx}, \\ q(x) &= p(x)\frac{a_0(x)}{a_2(x)}, \\ F(x) &= p(x)\frac{f(x)}{a_2(x)}. \end{aligned}$$

Using this notation, the Sturm-Liouville operator $\mathscr{L}$ can be defined as

$$\mathscr{L} = \frac{d}{dx}\left(p(x)\frac{d}{dx}\right) + q(x).$$

Next, writing this into an eigenvalue problem yields:

$$\mathscr{L}\phi_n = -\lambda_n \phi_n.$$

Here ϕ_n are the eigenfunctions and λ_n are the eigenvalues of the Sturm-Liouville operator $\mathscr{L}$. Hereby it is important to note that for each eigenvalue λ_n there exists an eigenfunction ϕ_n. Moreover, these eigenfunctions are nonzero and orthogonal, relative to each other.

3.2. Results and Analysis

In this section the results that are found by extending the differential equation presented by Chu[3] will be discussed. The extension looks at solutions to the nonlinear equation for bounded functions $F(u)$ that are not Lipschitz-continuous. Moreover, some numerical approximations of the solution to the system, for various functions $F(u)$, will be given. Finally, a stability analysis of the ODE (3.1) shall be preformed.

3.2.1. Solutions $u(t)$ for bounded $F(u)$

Consider a continuous function $F : X \to X$, where X is an Banach space and for each $u \in X$, $F(u)$ is bounded on X. From J.Chu [3] the solution to the system is given by.

$$u(t) = [\psi_0 - \omega] + \omega \tanh(t) + \int_t^\infty (s-t)\frac{F(u)}{\cosh^2(s)}\,ds$$

If $F(u)$ is bounded, then there exists $M \in \mathbb{R}^+$ such that for every $t \in [t_0, \infty)$ one has $|F(u(t))| \le M$. Therefore it is easy to see that

$$\begin{aligned} \left|\int_t^\infty (s-t)\frac{F(u)}{\cosh^2(s)}\,ds\right| &\le \int_t^\infty (s-t)\frac{|F(u)|}{\cosh^2(s)}\,ds \\ &\le \int_t^\infty \frac{(s-t)M}{\cosh^2(s)}\,ds \\ &= M(\ln(1+e^{-2t})) \end{aligned}$$

Which is clearly bounded by zero as $t \to \infty$. Moreover, it is bounded on its domain $[t_0, \infty)$, assuming $t_0 > -\infty$. This shows that for a bounded $F(u)$ there exists a real, physically valid, solution $u(t)$.

3.2.2. Numerical approximation of solutions to the nonlinear differential equation

The goal of this section is to find a numerical approximation of the solutions to the nonlinear differential equation (2.3), describing the Arctic gyre. Since it is not always the case that an analytical solution can be found for any $F(u)$, these numerical approximations can provide some insight into the behaviour of a solution. As stated in section 3.1.2, J.Chu[3] has presented a solution to equation (2.3), given by

$$u(t) = [\psi_0 - \omega] + \omega \tanh(t) + \int_t^\infty (s-t)\frac{F(u)}{\cosh^2(s)}ds. \tag{3.2}$$

To approximate this nonlinear equation, one can begin by assuming that there exists a bounded solution to equation (3.2) at t_0. By starting with a value $u_0(t) \in \mathbb{R}$, and defining

$$u_1(t) = [\psi_0 - \omega] + \omega \tanh(t) + \int_t^\infty (s-t)\frac{F(u_0)}{\cosh^2(s)}ds,$$

and similarly

$$u_{n+1}(t) = [\psi_0 - \omega] + \omega \tanh(t) + \int_t^\infty (s-t)\frac{F(u_n)}{\cosh^2(s)}ds$$

for a $n \in \mathbb{N}$. The code is able to find a fixed value for a specific $t \in [t_0.\infty)$, whenever $|u_{n+1} - u_n| < \epsilon$. Here $\epsilon \in \mathbb{R}$ is a constant, defining the tolerance.

To test this approach, the script is evaluated against some analytical solutions given by Jifeng Chu in "On a differential equation arising in geophysics" [2]. In this paper an analytical solution is presented for a constant oceanic vorticity, $F(u) = b$:

$$u(t) = [\psi_0 - \omega] + \omega \tanh(t) + b\ln(1 + e^{-2t})$$

where $b \in \mathbb{R}$. To visualise the numerical and analytical solution take

$$\omega = 4649.56, \quad \psi_0 = 0, \quad b = 1000.$$

Visualising $u(t)$ on the interval $t \in [0, 10)$ gives:

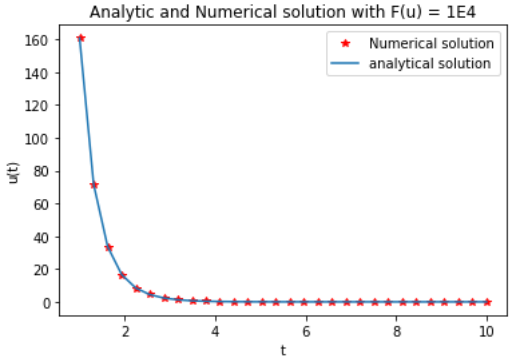

Figure 3.1: Analytical and numerical solution to $F(u) = 1000$

This graph illustrates that for constant values of $F(u)$, the numerical approximation gives similar values as the analytical solution.
For a more complex result, Chu's paper [2] presents the result for functions $F(u) = au$ where $a = -2$, formulated as

$$u(t) = -\frac{2\omega}{3}\tanh(t)\ln(\cosh(t)) + [\psi_0 + \omega]\tanh(t) - \frac{2\omega}{3} + \frac{2\omega}{3}t\tanh(t) + \frac{b}{2} - \frac{b}{2}\tanh(t) \quad t \geq 1 \tag{3.3}$$

However, note that for this solution $\lim_{t\to\infty} = \frac{\omega}{3}(1 - 2\ln(2)) + \psi_0$, instead of ψ_0. To correct this consider subtracting Chu's solution (3.3), by the constant $\frac{\omega}{3}(1 - 2\ln(2))$ to find:

$$u(t) = -\frac{2\omega}{3}\tanh(t)\ln(\cosh(t)) + [\psi_0 + \omega]\tanh(t) - \frac{2\omega}{3} + \frac{2\omega}{3}t\tanh(t) + \frac{b}{2} - \frac{b}{2}\tanh(t) - \frac{\omega}{3}(1 - 2\ln(2)). \tag{3.4}$$

For this equation the boundary conditions

$$\lim_{t\to\infty} u(t) = \psi_0 \qquad \lim t \to \infty \cosh(t)u'(t) = 0$$

hold. Moreover, inserting this back into the original differential equation (2.3) one finds that 3.2.2 gives a solution for $b = \frac{4\omega\ln(2)}{3} + \frac{2\omega}{3}$.
To visualise this, consider the same values for ψ_0 and ω on the interval $t \in [1,10]$, which produces the following graph:

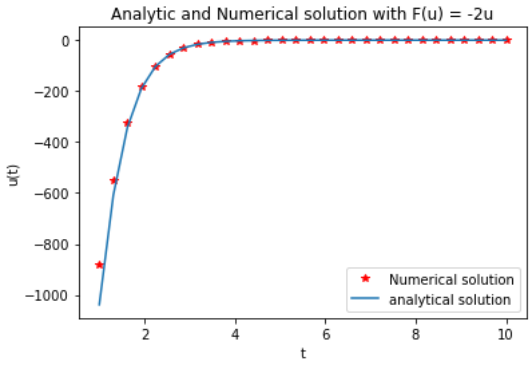

Figure 3.2: Analytic and numerical solution for F(u) = -2u

These plots illustrate that the algorithm can approximate the solution for some $F(u)$. From here, the claim that for every continuous function $F(u)$, the solution $u(t)$ has the condition $\lim_{t\to\infty} u(t) = \psi_0$, shall be visualised in figure (3.3).

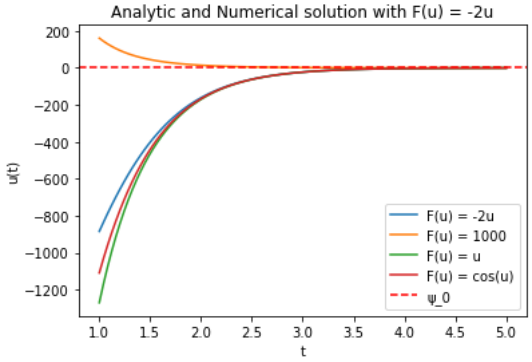

Figure 3.3: The numerical solutions of $u(t)$ for different values of $F(u)$, converging to ψ_0

Next, in section (3.2.1), a proof has been stated that the model has a result for bounded function of $F(u)$ that are not Lipschitz-Continuous. Therefore, consider the functions

$$F(u) = \sin(\frac{1}{u})$$

$$F(u) = \frac{1}{u} - \omega$$

Note that this function is bounded, but is not Lipschitz-continuous in $t \in [0,\infty)$. While it would be difficult to provide an analytic result to the differential equation in [3], a numerical approximation does give a result. This can be seen in figure (3.4).
These plots illustrate that the nonlinear differential equation presented in [3] can have solutions for periodic and Lipschitz-continuous functions, as well as functions of $F(u)$ that are only bounded.

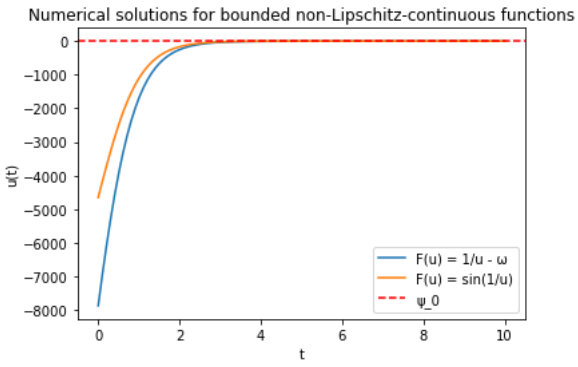

Figure 3.4: Numerical solution of $u(t)$ for $F(u) = sin(\frac{1}{u})$

3.3. Uniqueness of results for the nonlinear model

Writing the nonlinear dynamical system into a Sturm-Liouville eigenvalue problem can give some insight into the uniqueness and stability of the system. Consider the equation

$$u"(t) = \frac{\epsilon F(u)}{\cosh^2(t)} - \frac{2\omega \sinh(t)}{\cosh^3(t)}, \quad \epsilon \in \mathbb{R}, t \geq t_0$$

written as

$$u"(t) + \epsilon F(u)\frac{-1}{\cosh^2(t)} = -\frac{2\omega \sinh(t)}{\cosh^3(t)}$$

with the homogeneous form

$$u"(t) + \epsilon F(u)\frac{-1}{\cosh^2(t)} = 0. \tag{3.5}$$

Suppose $F(u) = u$, then the Sturm-Liouville operator is denoted as

$$\mathscr{L}(u) = \frac{d}{dt}(\frac{du}{dt}) + \epsilon \frac{-1}{\cosh^2(t)}u, \tag{3.6}$$

which results in the eigenvalue problem:

$$\phi_n"(t) + \epsilon \frac{-1}{\cosh^2(t)}\phi_n = \lambda_n \phi_n. \tag{3.7}$$

This eigenvalue problem turns out to be quite hard to solve analytically. Therefore one can apply a change of variables to rewrite it into a well studied problem. Consider the transformation:

$$t = \tanh(x)$$

which implies that,

$$\frac{1}{\cosh^2(t)} = 1 - \tanh^2(t) = 1 - x^2.$$

Applying the transformation to the derivatives:

$$\frac{du}{dt} = \frac{du}{dx}\frac{dx}{dt} = \frac{du}{dx}(1 - \tanh^2(t)) = \frac{du}{dx}(1 - x^2)$$

$$\frac{d^2u}{dt^2} = \frac{d^2u}{dx^2}\left(\frac{dx}{dt}\right)^2 + \frac{d^2x}{dt^2}\frac{du}{dx} = \frac{d^2u}{dx^2}(1 - x^2)^2 - 2x(1 - x^2)\frac{du}{dx}$$

Next, applying these changes to the homogeneous equation (3.5) gives

$$\frac{d^2u}{dx^2}(1 - x^2)^2 - 2x(1 - x^2)\frac{du}{dx} + (\epsilon x^2 - \epsilon)u = 0 \tag{3.8}$$

or in simplified terms

$$\left(1-x^2\right)\left(\frac{d^2u}{dx^2}(1-x^2)-2x\frac{du}{dx}-\epsilon u\right)=0$$

For this problem, take $x \neq \pm 1$, such that the non trivial case is considered where

$$\frac{d^2u}{dx^2}(1-x^2)-2x\frac{du}{dx}-\epsilon u=0 \tag{3.9}$$

Rewriting equation (3.9) in to a Sturm-Liouville eigenvalue problem

$$(p(x)V')'+q(x)V=\lambda V$$

using

$$p(x)=e^{\int \frac{-2x}{1-x^2}dx}=x^2-1$$

$$q(x)=(x^2-1)\left(\frac{-\epsilon}{1-x^2}\right)=\epsilon$$

provides

$$((x^2-1)V')'=(\lambda-\epsilon)V. \tag{3.10}$$

Now that the problem has been transformed into a Sturm-Liouville eigenvalue problem, one can try to solve this differential equation by relating it to a problem with a known solution. Therefore consider the Legendre equation [5]

$$-((1-x^2)y'(x))'+\frac{\mu^2}{1-x^2}y(x)=\lambda y(x) \quad \text{for all } x\in(-1,1).$$

Taking $\mu=0$ and $\bar{\lambda}=\lambda-\epsilon$, the Legendre equation equals the homogeneous differential equation used to describe the Arctic gyre. For $\mu=0$, the spectral parameter is given by[5]:

$$\bar{\lambda_n}=n(n+1)$$

such that

$$\lambda_n=n(n+1)+\epsilon \tag{3.11}$$

are eigenvalues of equation (3.5). This shows that setting parameter $\epsilon>0$ implies that all eigenvalues of the differential equation are greater than zero. Therefore that the system only emits unstable solutions when scaling by such a parameter. Extending the problem for linear functions of $F(u)$, namely $F(u)=au+b$, gives similar results. As the Sturm-Liouville eigenvalue problems considers the homogeneous form, the same transformation can be taken to arrive at

$$((x^2-1)V')'=(\lambda-a\epsilon)V. \tag{3.12}$$

This yields eigenvalues

Similarly, there exist no stable solutions when $\epsilon>-\frac{n(n+1)}{a}$, for any $n\in\mathbb{N}$. From here, the question arises whether or not solutions can be unique.

3.3.1. Existence of solutions when scaling $F(u)$ by ϵ

As seen in the previous section, the eigenvalues to the nonlinear differential equation 3.1 are given by $\lambda_n=n(n+1)+\epsilon$. Considering the case where $\epsilon\leq 0$, such that there exists a $\lambda=0$. Then the Fredholm alternative states that there exists a unique solution to the differential equation (3.1) if

$$\int_t^\infty f(x)\phi(x)dx=0,$$

where $f(x) = \frac{2\omega\sinh(x)}{\cosh^3(x)}$ and $\phi(x)$ is the eigenfunction corresponding to $\lambda = 0$. Suppose that there exists an $\epsilon \in \mathbb{R}$ such that, for an $n \in \mathbb{N}$, $\lambda_n = 0$. Then the Sturm-Liouville eigenvalue problem (3.10) turns into

$$((x^2-1)V')' = 0.$$

Using simple analysis this can be written as

$$(x^2-1)V' = A \quad \text{and} \quad V' = \frac{A}{x^2-1} = \frac{A}{2}\left(\frac{1}{1-x} + \frac{1}{1+x}\right)$$

which implies

$$V = \frac{A}{2}\ln\left(\frac{1+x}{1-x}\right) + B$$

for $A, B \in \mathbb{R}$

This provides an eigenfunction in terms of the original variable t by rewriting $x = \tanh(t)$:

$$\phi(t) = \frac{A}{2}\ln\left(\frac{1+x}{1-x}\right) + B = \frac{A}{2}\ln\left(\frac{1+\tanh(t)}{1-\tanh(t)}\right) + B$$

Using the Fredholm Alternative, there exists a solution if

$$\int_t^\infty \left(\frac{2\omega\sinh(s)}{\cosh^3(s)}\right)\left(\frac{A}{2}\ln\left(\frac{1+\tanh(s)}{1-\tanh(s)}\right) + B\right) ds = 0$$

For an arbitrary $t \in \mathbb{R}$ this yield quite and elaborate result. Therefore consider $t_0 = 0$, such that the integral converges to

$$\int_0^\infty \left(\frac{2\omega\sinh(s)}{\cosh^3(s)}\right)\left(\frac{A}{2}\ln\left(\frac{1+\tanh(s)}{1-\tanh(s)}\right) + B\right) ds = (A+B)\omega.$$

This results shows that there only exists a solution to the differential equation if $A = -B$. Note that the boundary conditions to the differential equation are $\lim_{t\to\infty} u(t) = \psi_0$ and $\lim_{t\to\infty} \cosh(t)u'(t) = 0$. However, it shows that for all $A, B \in \mathbb{R}$, the $\lim_{t\to\infty} \phi(t)$ diverges. Using the mathematical software "Maple", it shows that this is the case for any $t_0 \in \mathbb{R}$. This concludes that there exist no unique solution to the differential equation if $\epsilon = -n(n+1)$, for any $n \in \mathbb{N}$.
Similarly for linear function $F(u) = au + b$, where $a, b \in \mathbb{R}$ are constants, the integral

$$\int_t^\infty \left(\frac{2\omega\sinh(s)}{\cosh^3(s)} - \frac{b}{\cosh^2(s)}\right)\left(\frac{A}{2}\ln\left(\frac{1+\tanh(s)}{1-\tanh(s)}\right) + B\right) ds = 0$$

poses no unique solutions for eigenfunctions that hold for the original boundary conditions.
To summarise, equation 3.1 has unique solutions if $\epsilon \neq -\frac{n(n+1)}{\alpha}$, for α nonzero.

4

Conclusion and Discussion

The following sections will discuss the primary conclusions drawn from this report. It will address potential limitations, and suggest directions for future research. By doing so, the existing model presented by Jifeng Chu[3] can be expanded such that there exists a more detailed approach to model the Arctic gyre.

4.1. Conclusion

The study of Arctic gyres, large systems of circulating ocean currents formed by wind patterns and the Earth's rotation, is crucial due to their significant role in global climate. These gyres redistribute heat from the Equator to the poles and facilitate the exchange of nutrients and gases between the ocean and atmosphere [9]. The unique properties of Arctic gyres make it a well studied topic. Understanding these dynamic systems is essential for comprehending the effect that these gyres can have.

This report dives into the nonlinear model for Arctic gyres presented by Jifeng Chu[3], exploring and understanding its mathematical formulations, and extending its applications. The model Chu presents is based on a model presented by Constantin and Johnson[4] who derive a two-dimensional ordinary differential equation, using the stereographic projection, describing the gyre. In the specific case, simplifying the model by neglecting azimuthal variations results in a second order nonlinear differential equation. This offers a manageable approach to studying the dynamics of the system. In this report, the extension of Chu's work involved researching different properties of the non-linear model for various functions $F(u)$ representing oceanic vorticity. Furthermore the stability and uniqueness of the model has been analysed by rewriting the system into a Sturm-Liouville eigenvalue problem, and applying Fredholm's alternative, in the case of eigenvalues that are zero.

The presented model has unique continuous solutions $u : [t_0, \infty) \to \mathbb{R}$ if the oceanic vorticity function $F(u)$ is Lipschitz-continuous. The findings in this report indicate that the model has continuous solutions for bounded functions of $F(u)$, even if $F(u)$ is not Lipschitz-continuous function. Additionally, numerical approximations validated against analytical results confirm that the model eventually converges to ψ_0, a specific starting parameter describing the initial vorticity. Moreover, these numerical methods give light to the possibility of the use of vorticity functions $F(u)$ that are not-Lipschitz-Continuous. Moreover, it has been shown that for linear function $F(u) = au + b$, where $a, b \in \mathbb{R}$, there exist no unique solutions to the system describing the vorticity of the Arctic gyre, if $\epsilon = \frac{n(n+1)}{a}$, for any $n \in \mathbb{N}$.

The exploration in this report underscores the importance of accurately modeling of Arctic gyres. The extensive understanding of this model, its parameters and its stability gives a manageable and comprehensive model of Arctic gyres. Future work should focus on addressing the intricate behaviors of ocean dynamics through the use of non-Lipschitz continuous functions. By doing so the model can better predict and mitigate the impacts of gyres on global climate patterns and marine ecosystems.

4.2. Discussion

This study delved into the non-linear model for Arctic gyres, focusing on its extension, stability, and bifurcation analysis. While the findings provide valuable insights, there are several limitations and areas for further exploration.

4.2.1. Numerical Divergence

One of the primary shortcomings of the numerical model is its struggle with approximating a solution for values if $t \to \infty$. The fact that these values can approach infinity is an aspect that is derived form using the stereographic projection. Since water in the gyre moves closer to the North Pole, the projection will be stretched out infinitely. In the numerical approximation of the integral, it mostly showed that around $\underset{.}{t} = 5$ the value of the solution is already quite close to ψ_0. This can be the result of the numerical approximation of $\frac{1}{\cosh^2(t)}$ that decease exponentially to zero. It is possible that the python module converts this to quickly to zero as t grows. A solution for this could be taking a different approach then the fixed point iteration, or using an approximation of $\cosh^2(t)$. Moreover, the numerical approximation of indefinite integrals poses potential errors, particularly in ensuring the stability and convergence of the solutions over an unbounded domain. The reliance on an expected fixed value for the function u(t) over a large but finite interval can introduce inaccuracies. Therefore, improving the numerical methods, such as implementing more sophisticated integration techniques or adaptive mesh refinement, could mitigate these issues and lead to more reliable results.

4.2.2. Simplification of the model

The simplified model, while useful for initial analysis, may not fully capture the complexities of real-world ocean dynamics. For instance, the model assumes no azimuthal variation and simplifies the flow to a radially symmetric function. These assumptions may overlook critical factors such as transient effects, non-uniform ocean bottom formation, and variable external forces, which are all influential in real oceanic systems. To create a more realistic result, extension and further research of the model could incorperate these complexities.

A

Python model of fixed point integration for different F(u)

This appendix states the python code that is used to numerically analyse the solution to the ODE.

A.1. Python Code

```
# -*- coding: utf-8 -*-
"""
Created on Tue Jun 11 16:13:49 2024

@author: sever
"""

# -*- coding: utf-8 -*-
"""
Created on Mon May 27 10:06:37 2024

@author: sever
"""

import matplotlib.pyplot as plt
import numpy as np
from scipy.integrate import quad


omega = 4649.56
psi_0 = 0

#define function of F(u):


def F(u):

    return u
    # return 10000

def integrand(u,s,t):
    return (s-t)*F(u)/(np.cosh(s)**2)
```

```
def u_t(t,u_iter):
    res, err = quad(lambda s: integrand(u_iter, s,t),t,np.inf)
    return psi_0 - omega + omega*np.tanh(t) + res

def approx_u(t, init = omega/2, tol = 1E-4, max_iterations = int(1E4)):
    res = np.array([init])
    u_iter = init
    for i in range(max_iterations):
        u_new = u_t(t, u_iter)
        res = np.append(res,u_new)
        if np.abs(res[-1]-res[-2]) < tol:
            return u_new

        u_iter = res[-1]
    raise ValueError("Fixed-point iteration did not converge within tolerence")


t_vals = np.linspace(0,10,100)
u_vals = [approx_u(t) for t in t_vals]



def analytical_sol(t):
    b = 4*omega*np.log(2)/3 + 2*omega/3
    # b= 10000
    C = (omega/3)*(1+2*np.log(2))
    return (-2*omega*np.tanh(t)/3)*np.log(np.cosh(t)) + (psi_0+omega)*np.tanh(t) + 2/3 *
    (-omega + omega*t*np.tanh(t)) +(b/2)*(1-np.tanh(t))-C
    # return psi_0 - omega + omega*np.tanh(t)+b*np.log(1+np.exp(-2*t))



# def F(u):

#     return -2*u

# u_vals = [approx_u(t) for t in t_vals]
# plt.plot(t_vals, u_vals, label= "F(u) = -2u")



# def F(u):

#     return 1E4

# u_vals = [approx_u(t) for t in t_vals]
# plt.plot(t_vals, u_vals, label= "F(u) = 1000")


# def F(u):

#     return u

# u_vals = [approx_u(t) for t in t_vals]
# plt.plot(t_vals, u_vals, label= "F(u) = u")
```

```
def F(u):

    return np.sin(1/u)

u_vals = [approx_u(t) for t in t_vals]
plt.plot(t_vals, u_vals, label= "F(u) = sin(1/u)")


# plt.plot(t_vals,analytical_sol(t_vals), label = "analytical solution")
plt.xlabel('t')
plt.ylabel('u(t)')
plt.axhline(y = psi_0,color = "r", linestyle = "--", label = "\u03C8_0")
plt.title("Numerical solutions F(u)= sin(1/u)")
plt.legend()
plt.show()
```

B

Proofs and results outside the scope of the project

In this report, some proofs or equations were simplified, due to there complicated and extensive nature. This appendix showcases some of these results.

B.1. Eigenfunction solution for arbitrary t

Solving for eigenfunctions if $F(u) = u$ for an arbitrary t in "Maple" gives:

$$\int_t^\infty \left(\frac{2\omega \sinh(s)}{\cosh^3(s)} \frac{A}{2} \ln\left(\frac{1+\tanh(s)}{1-\tanh(s)} \right) + B \right) ds$$

$$= -\frac{1}{2}\omega \left(IA\pi \operatorname{csgn}(Ie^t) \operatorname{csgn}(Ie^{2t}) e^{2t} - 2IA\pi \operatorname{csgn}(Ie^t) \operatorname{csgn}(Ie^{2t})^2 e^{2t} + IA\pi \operatorname{csgn}(Ie^{2t})^3 e^{2t} - 4Ae^{2t} \ln(e^t) - 2Ae^{2t} - 4Be^{2t} - 2A \right)$$

Which is equal to zero if:

$$A = \frac{-\left[4IBe^{2t}\omega + (e^{2t})^2 + 2e^{2t} + 1 \right]}{\left[\omega\pi \operatorname{csgn}(Ie^t)^2 \operatorname{csgn}(Ie^{2t}) e^{2t} - 2\pi \operatorname{csgn}(Ie^t) \operatorname{csgn}(Ie^{2t})^2 e^{2t} + \pi \operatorname{csgn}(Ie^{2t})^3 e^{2t} + 4Ie^{2t} \ln(e^t) + 2Ie^{2t} + 2I \right]}$$

The same principle holds for all linear function $F(u) = au + b$. Then

$$\int_t^\infty \left(\frac{2\omega \sinh(s)}{\cosh^3(s)} - \frac{b}{\cosh^2(s)} \right) \left(\ln\left(\frac{A}{2} \frac{1+\tanh(s)}{1-\tanh(s)} \right) + B \right) ds = 0$$

must hold.

Taking the limit of $t \to \infty$ of the latter equation diverges, independent of the variable B. Therefore the solution can not hold for the boundary condition. Thus there are no solutions to the problem if $\epsilon = -\frac{n(n+1)}{a}$.

Bibliography

[1] Vorticity, n.d. URL https://www.sciencedirect.com/topics/engineering/vorticity. Accessed: 2024-06-03.

[2] Jifeng Chu. On a differential equation arising in geophysics. *Monatshefte für Mathematik*, 187(3):499–508, 2018. doi: 10.1007/s00605-017-1087-1. URL https://doi.org/10.1007/s00605-017-1087-1.

[3] Jifeng Chu. On a nonlinear model for arctic gyres. *Annali di Matematica Pura ed Applicata (1923 -)*, 197(2):651–659, 2018. doi: 10.1007/s10231-017-0696-6. URL https://doi.org/10.1007/s10231-017-0696-6.

[4] Adrian Constantin and Roger S. Johnson. Large gyres as a shallow-water asymptotic solution of euler's equation in spherical coordinates. *Proceedings of the Royal Society A: Mathematical, Physical and Engineering Sciences*, 473(2200):20170063, 2017.

[5] W. Norrie Everitt. Sturm-liouville theory: Past and present. In *Sturm-Liouville Theory: Past and Present*, pages 271–331. Birkhäuser Verlag Basel/Switzerland, 2005. Retrieved from path_to_your_uploaded_pdf.

[6] Susanna V Haziot and Kateryna Marynets. Applying the stereographic projection to modeling of the flow of the antarctic circumpolar current. *Oceanography*, 31(3):68–75, 2018. doi: 10.5670/oceanog.2018.311. URL https://doi.org/10.5670/oceanog.2018.311.

[7] National Geographic Society. Coriolis effect, 2023. URL https://education.nationalgeographic.org/resource/coriolis-effect-1/. Accessed: 2024-06-12.

[8] Norwegian University of Science and Technology. Banach spaces lecture notes, 2020. URL https://wiki.math.ntnu.no/_media/tma4145/2020h/banach.pdf. Accessed: 2024-06-03.

[9] National Geographic Society. Ocean gyre, 2024. URL https://education.nationalgeographic.org/resource/ocean-gyre/. Accessed: 2024-06-04.